

Original Article

## Weeds detection in saffron fields using an improved YOLOv5 model

Roghaieh Shamloo, Alireza Soleimanipour\*, Abbas Rezaei Asl

Department of Biosystem Engineering, Gorgan University of Agricultural Sciences and Natural Resources, Gorgan, Iran

Biosystems Engineering and Renewable Energies 2025, 1 (1): 44-50

### KEYWORDS

Deep learning  
Object detection  
Saffron  
Weeds control  
YOLOv5

\* Corresponding author  
asoleimani@gau.ac.ir

### Article history

Received: 2024-11-27  
Revised: 2025-2-3  
Accepted: 2025-2-4

### ABSTRACT

The excessive use of agricultural pesticides and inputs has caused severe environmental damage to agricultural ecosystems. By applying digital agriculture and variable rate application systems, various sections of a farm can be managed with varying levels of pesticides and inputs, which is beneficial both in terms of production costs and environmental issues. In this study, a weed and saffron plant detection model was designed and evaluated to develop a selective weed control system in saffron fields. The proposed weed detection model is based on the YOLOv5 object detection model. Several CBS and C3 modules in the YOLOv5s model were replaced with Ghost Bottleneck and C3Ghost modules, respectively. This was done to reduce the number of model parameters and make the network lighter, which increases the speed of image processing during model training and inference. Furthermore, to improve the detection accuracy of the proposed model, a coordinate attention (CoordAtt) layer was used. The results showed that the number of parameters in the proposed model was reduced by 47% compared to the corresponding model in terms of network width and depth coefficients in YOLOv5 versions. Meanwhile, among the six trained models, the modified YOLOv5s model demonstrated the best performance, achieving accuracy and recall values equal to 81% and 67%, respectively. The detection accuracy of the proposed model was 3.93% higher than that of the best-performing YOLOv5 algorithm. Due to the lightweight nature of the proposed algorithm, it can be used for real-time weed detection in agricultural fields to develop selective control systems.

Abbreviation	Description
BatchNorm	Batch Normalization layer
C3	A CSP bottleneck that includes 3 convolutional layers
C3Ghost	A convolutional block composed from the integration of Ghost modules into the C3 structure
CBS	Convolution-BatchNorm-SiLU
Conv	Convolution layer
CoordAtt	Coordinate Attention
CSP	Cross Stage Partial layer
FN	False Negative
FP	False Positive
mAP	mean Average Precision
mAP50	mean Average Precision at an Intersection over Union (IoU) threshold of 0.50
mAP50-95	mean Average Precision averaged across Intersection over Union (IoU) thresholds from 0.50 to 0.95
SiLU	Sigmoid-Weighted Linear Unit
SPP	Spatial Pyramid Pooling
SPPF	Spatial Pyramid Pooling - Fast
TN	True Negative
TP	True Positive
VRA	Variable Rate Application
VRAM	Video RAM
YOLO	You Only Look Once
Yolov5	5 <sup>th</sup> version of the YOLO model
Yolov5l	Large-scale of the Yolov5 model
Yolov5m	Medium-scale of the Yolov5 model
Yolov5n	Nano-scale of the Yolov5 model
Yolov5s	Small-scale of the Yolov5 model
Yolov5x	Extra Large-scale of the Yolov5 model

## 1. Introduction

The growing global population and the pressing need to ensure access to healthy food for all, combined with limited water resources and arable land, require effective strategies to enhance crop yield and quality per unit area. However, the indiscriminate use of agricultural pesticides and inputs has caused significant environmental harm to agricultural ecosystems. These challenges, along with water scarcity and the need to conserve energy for sustainable development, highlight the importance of adopting innovative approaches and advanced technologies in designing agricultural tools and machinery (Admasu et al., 2024). Among the most promising advancements in agriculture are artificial intelligence and robotics, particularly in the field of digital farming. Digital farming, including variable rate application (VRA) systems, enables precise management of different farm sections by varying pesticide or input levels, leading to reduced production costs and a lower environmental footprint (Zhou et al., 2023).

Saffron (*Crocus sativus* L.) is a perennial herbaceous plant characterized by its bulb, leaves, petals, stigma, and stamens. Its primary product is the red stigma, which is dried during processing to produce saffron. With a history spanning over 2,500 years as a medicinal plant, saffron was recognized in the European Pharmacopoeia from the 16th to the 20th centuries (José Bagur et al., 2017). It contains more than 300 volatile and non-volatile compounds, including safranal, picrocrocin, crocin, monoterpene glycosides, aldehydes, and various carotenoids, all of which contribute to its medicinal properties. Known as the world's most expensive spice and often referred to as "red gold" (Fernández, 2004), saffron is cultivated in regions of the

Mediterranean, Europe, and Asia. Among these, Iran stands out as the largest producer, with the most extensive saffron cultivation area globally (Shahnoushi et al., 2020). According to the latest statistics from Iran's Ministry of Agriculture (Ministry of Agriculture-Jihad, 2020), the country has over 120,000 hectares of saffron cultivation, producing 439,000 kg in 2020.

The high cost of saffron is primarily due to its low yield per hectare and the labor-intensive nature of its cultivation, maintenance, harvesting, and processing (Kumar et al., 2008). Traditional agricultural practices, combined with the lack of appropriate machinery for saffron production, mean that a significant portion of the work is done manually. As a result, some producers neglect essential tasks such as pest, disease, and weed control, despite their critical impact on crop yield and quality. In recent decades, the global demand for saffron has risen significantly due to its nutritional and medicinal value, reflecting growing consumer interest worldwide (Abdullaev and Frenkel, 1999).

Weeds remain a persistent challenge for farmers, competing with crops for water, soil nutrients, sunlight, and space, while also providing habitats for pests and diseases. This competition weakens plants and reduces crop yields (Cheng and Matson, 2015; Singh et al., 2016). To combat this, farmers employ various weed control methods, including agricultural practices, plant quarantine, hand weeding, biological control, and chemical control (Woyessa, 2022). In saffron cultivation, weed control is particularly critical, as weeds cause more damage than other pests or diseases. However, traditional weed management methods are labor-intensive and expensive. Chemical control, involving indiscriminate herbicide spraying across fields, further increases costs and poses environmental risks. Excessive herbicide use in agriculture contributes to pollution, as highlighted by the European Food Safety Authority, which found that 98.9% of food products contain agricultural chemical residues, with 1.5% exceeding safe limits (Rodrigo et al., 2014). Overuse of herbicides has also led to the development of herbicide-resistant weeds, a growing threat to crop production worldwide (Jeanmart et al., 2016). In response, many European countries have begun restricting herbicide use in agriculture (Hamuda et al., 2016). To address these challenges, researchers have developed alternative weed control methods in recent years. For instance, a study demonstrated the effectiveness of spot spraying to target weeds in corn fields, reducing the reliance on widespread herbicide application (Guerrero et al., 2017).

Our objective in this research is to present a solution for implementing selective weed control in saffron fields. This solution involves real-time detection of weeds in the field and subsequent targeted application of herbicides. To achieve this, a lightweight object detection model based on Yolov5 is proposed for weed detection. By replacing certain components of the Yolov5 architecture with lighter modules, we have developed a model that can be used in real-time applications while maintaining high accuracy. Integrating this model with a variable-rate sprayer enables targeted herbicide application only in areas infested with weeds.

## 2. Materials and Methods

### 2.1. Image dataset

Saffron plants were cultivated in rows, with approximately 25 cm of spacing between rows and less than 25 cm between plants within a row. Weed control began during the early growth stages, known as the two-leaf or multi-leaf stage, as the saffron plant cannot effectively compete with weeds at this time. To train and evaluate the model developed in this work, images were collected during this critical growth stage. A total of 620 images were captured at various times of the day in a saffron field located in Azadshahr County, Golestan Province, Iran. The images were taken with a smartphone camera (Xiaomi Redmi Note 9S) held perpendicular to the field surface, relying on natural ambient

light without artificial illumination. To account for different lighting conditions, images were taken in the morning, noon, and afternoon. The image content consists of saffron cultivation rows, potentially contaminated by various weed species, including broad-leaved and thin-leaved grasses (Figure 1). The original images had a resolution of 3000×3000 pixels. To optimize them for the Yolov5 object detection model, the resolution was reduced to 640×640 pixels. Using the labellmg software, saffron plants and weeds within the images were annotated. In total, 6000 objects were labeled, with approximately 68% identified as saffron plants and the rest as weeds. The annotation process was conducted by a skilled person, knowledgeable about the shapes and characteristics of saffron plants and weeds. A sample of the annotated images is shown in Figure 1.

### 2.2. Yolov5 architecture

The YOLO algorithm is renowned for its speed in object detection. Initially introduced by Redmon (2016), YOLO has consistently demonstrated superior performance among single-stage object detection algorithms. Since then, several versions of YOLO have been released, from YOLO v1 to YOLO v8, as well as YOLOR and YOLOX. These versions have been adapted by researchers to suit specific datasets and applications. Of these, Yolov5 has seen the most modifications due to its simplicity and strong performance. Enhanced versions of Yolov5 have been proposed for a wide range of applications, from medical to agricultural fields. In this study, we present a modified version of the Yolov5n architecture tailored for weed detection in saffron fields, designed for real-time application.

The YOLO algorithm architecture is typically divided into three components: the backbone, the neck, and the head. The backbone is responsible for extracting features from the input images. The neck then fuses these extracted features. Finally, the head performs the prediction operation, which is a type of regression. Figure 2 illustrates the architecture of the Yolov5 algorithm.

Yolov5 is available in five different scales, each with varying network depth and width multipliers: Yolov5n (nano), Yolov5s (small), Yolov5m (medium), Yolov5l (large), and Yolov5x (extra-large). As the scale increases from nano to extra-large; the model size, number of layers, and parameters also increase, typically improving performance in larger models but also slowing down training and inference speeds. The choice of the most suitable model depends on the specific application and available hardware. Table 1 outlines the configuration of each scale, including the depth and width multipliers.

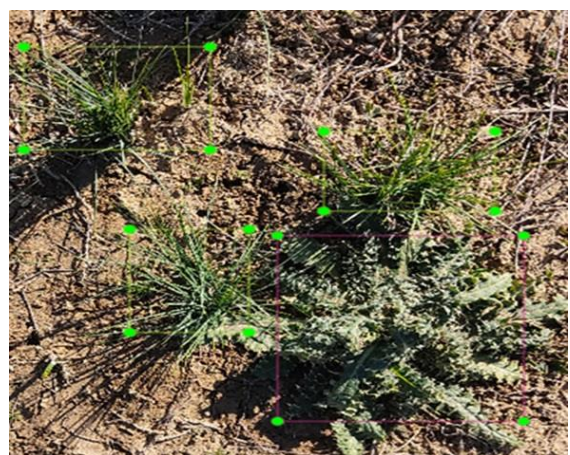


**Figure 1.** Sample annotated image using labellmg software (Green: Saffron plant, Purple: Weed)

**Table 1.** Configuration of YOLO models with different scales

Model scale	n	s	m	l	x
depth multiple	0.33	0.33	0.67	1.00	1.33
width multiple	0.25	0.5	0.75	1.00	1.25

The architecture of Yolov5 remains consistent across all the scales mentioned and follows the structure depicted in Figure 2. The backbone is mainly composed of CBS, C3, and SPPF modules, with the structure of these modules illustrated in Figure 3. The CBS module consists of three layers: a convolutional layer (Conv), a batch normalization layer (BatchNorm), and a SiLU activation layer. The C3 module divides the feature map from the base layer

into two parts and then merges them using an intermediate-level hierarchy, which helps eliminate redundant computations caused by repetitive image gradient information. This enhances the model's trainability and reduces computational costs. The SPPF module is an upgraded version of the Spatial Pyramid Pooling (SPP) module, enabling it to convert feature maps of varying sizes into a fixed-size feature vector.

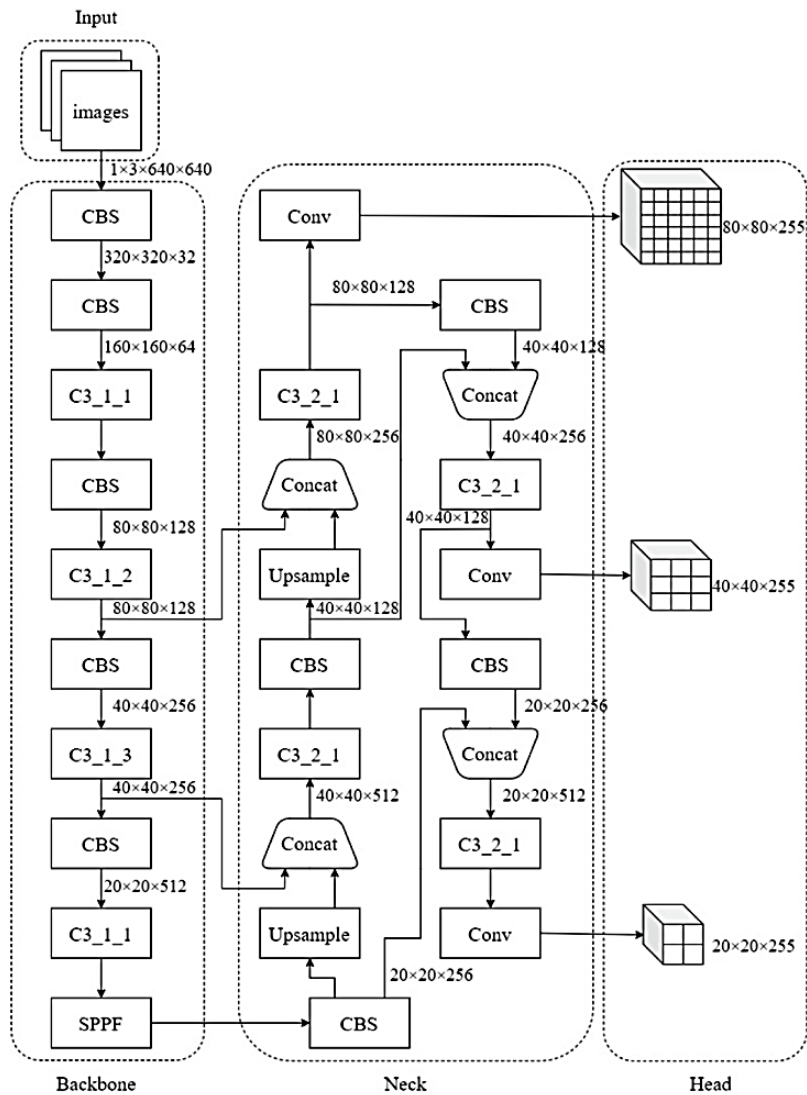


Figure 2. Network architecture of the Yolov5 model

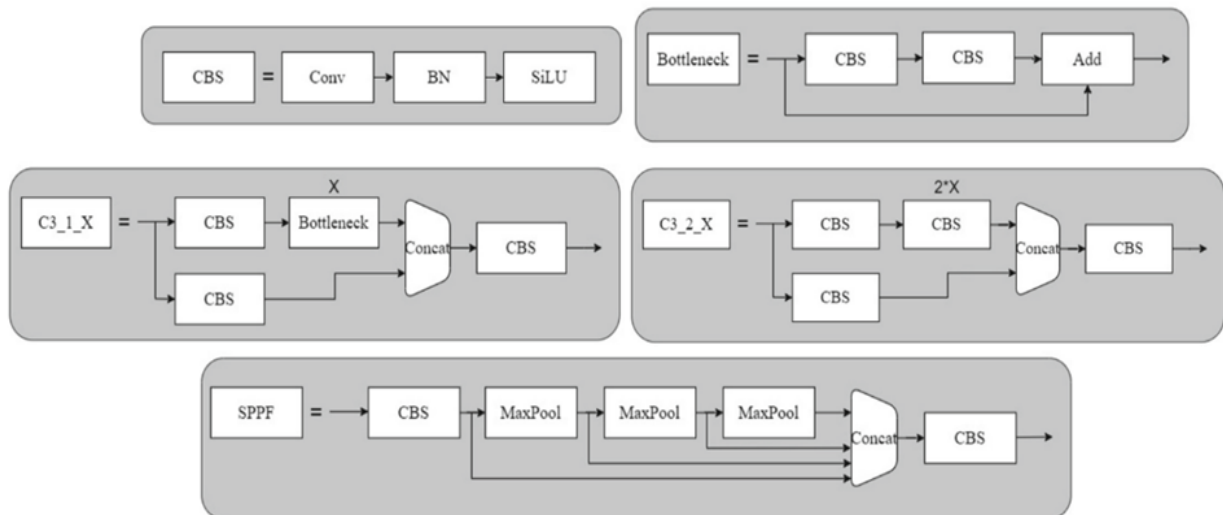


Figure 3. The structure of the CBS, Bottleneck, C3, and SPPF modules

### 2.3. The architecture of the improved Yolov5

Deep convolutional neural networks typically consist of tens or even hundreds of layers, along with a large number of parameters. While increasing the number of layers and parameters can improve feature extraction—provided that issues, like gradient vanishing and exploding, are mitigated—there are practical limitations due to memory size and the computational power needed for model training and deployment. As a result, efforts are focused on developing object detection models that balance high detection accuracy with being computationally lightweight and easier to deploy. To address these challenges, the proposed improved Yolov5 algorithm incorporates Ghost Bottleneck and C3Ghost modules, replacing the CBS and C3 modules, respectively. This substitution results in a lighter Yolov5 model by reducing the number of parameters and computational costs for both training and inference. Additionally, a coordinate attention mechanism module is introduced to enhance the network's feature extraction capabilities and improve model performance. It is positioned in the backbone, just before the SPPF module (Figure 4).

A Ghost Bottleneck is a skip connection block, similar to the basic residual block in ResNet in which several convolutional layers and shortcuts are integrated, but stacks Ghost Modules instead (two stacked Ghost modules). It was proposed as part of the GhostNet CNN architecture. A Ghost Bottleneck typically consists of two stacked Ghost Modules. The first module expands the number of channels, determined by the expansion ratio. The second module reduces the number of channels to match the shortcut connection. This shortcut connects the input directly to the output of both Ghost Modules. Batch normalization (BN) and ReLU activation are applied after each layer within the bottleneck (Han et al., 2020).

The CoordAtt mechanism is an innovative attention module that effectively captures both channel relationships and positional information within feature maps. Unlike previous methods like squeeze-and-excitation (SE) that primarily focused on channel dependencies, CoordAtt explicitly encodes spatial information by separately pooling features along the horizontal and vertical dimensions. This generates two 1D feature vectors per channel, capturing the distribution of features across these spatial directions. These vectors are then concatenated and processed by a 1x1 convolutional layer to generate attention weights for each channel, considering both horizontal and vertical positional information. Finally, these attention weights are reshaped and broadcast to refine the original feature map by emphasizing regions deemed important based on both channel and spatial cues. This unique approach allows CoordAtt to selectively focus on relevant regions within the input data, significantly improving the performance of deep learning models in various computer vision tasks while maintaining computational efficiency (Hou et al., 2021).

### 2.4. Training of the improved Yolov5

The collected image dataset was split into training and testing sets in an 80:20 ratio, resulting in 496 images for training each model and 124 images for evaluating the models. The proposed model was implemented using the PyTorch framework. Both the proposed model and the Yolov5 models with different scales were trained on the training images using a high-performance computer equipped with an NVIDIA® GeForce RTX™ 4080 graphics card (16 GB of VRAM), an Intel® Core™ i5-13600KF processor, 32 GB of RAM, and the Windows 11 operating system. The batch size was set to 16, and the number of training epochs was set to 200. All other hyperparameters were left at their default values.

### 2.5. Performance evaluation criteria

The models were evaluated based on the metrics of Precision (Eq. 1), Recall (Eq. 2), average precision (AP) (Eq. 3), and mean AP (mAP) (Eq. 4)

$$\text{Precision} = \frac{TP}{TP + FP} \quad (1)$$

$$\text{Recall} = \frac{TP}{TP + FN} \quad (2)$$

$$\text{AP} = \int_0^1 P dR \quad (3)$$

$$\text{mAP} = \frac{1}{n} \sum_{i=0}^n \text{AP}_i \quad (4)$$

where, TP is true positives, showing the number of objects correctly identified, FP is false positives, showing the number of objects that are not present in the image but are incorrectly identified as objects, FN is false negatives, determining the number of objects that are present in the image but are incorrectly not identified, and finally, AP is the area under the precision-recall curve.

## 3. Results and Discussion

This study presents an object detection model based on improved Yolov5s for identifying weeds and saffron plants in a saffron field. To reduce the number of parameters in the original Yolov5s model, Ghost Bottleneck and C3Ghost modules were integrated. Additionally, a CoordAtt module was added to the model architecture. To evaluate the performance of the proposed model and compare it with existing Yolov5 variants, the model, along with five other Yolov5 models (Yolov5n, Yolov5s, Yolov5m, Yolov5l, and Yolov5x), was trained on images captured from a saffron field.

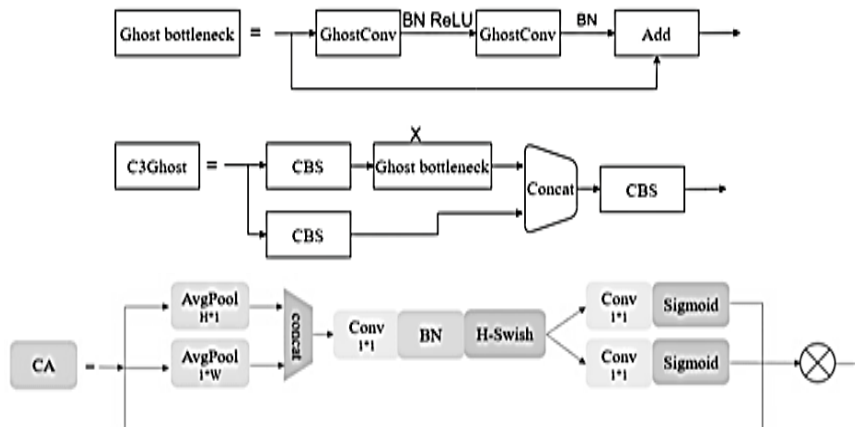


Figure 4. Network structure of the Ghost Bottleneck, C3Ghost, and CoordAtt modules used in the improved Yolov5 model

The evaluation results, including precision, recall, mean Average Precision at 50% Intersection over Union (mAP50), and mean Average Precision across 50% to 95% Intersection over Union thresholds (mAP50-95), are summarized in Table 2. The table also includes details on the number of layers and parameters for each trained model. As shown in Table 2, Yolov5n and Yolov5s have fewer network layers compared to the other models. Since both share the same width multiples, their layer count is identical. Although the number of layers in the improved model has increased due to the incorporation of different modules in its architecture, it has fewer parameters than its counterpart with the same width and depth multiples, the Yolov5s model. Notably, the proposed model reduces the number of parameters by 47%. This reduction translates to a smaller model size and faster performance when evaluating test images. The proposed model demonstrated superior accuracy and recall compared to the other trained models. Specifically, it achieved a 3.93% improvement in accuracy and a 1.01% improvement in recall over the Yolov5m model, which had the highest performance among the Yolov5 variants. The performance improvement is even more pronounced when compared to the Yolov5 model with the same width and depth multipliers.

A precision-recall curve illustrates the trade-off between precision (the proportion of true positives among all predicted positives) and recall (the proportion of true positives identified out of all actual positives) at various classification thresholds. Figure 5 presents the precision-recall curves for saffron plant and weed detection. Notably, the curve for saffron plant detection consistently lies above the curve for weed detection across a range of recall levels. This observation indicates that the proposed model exhibits higher precision in identifying saffron plants compared to weeds at equivalent recall values. In essence, the model demonstrates a stronger ability to correctly classify saffron plants as saffron plants while maintaining a similar level

of sensitivity in detecting both classes. This disparity in performance can likely be attributed to the class imbalance observed in the training dataset, where saffron plant samples may have been more abundant than weed samples. A larger number of training examples for saffron plants would naturally provide the model with more robust learning signals and better generalization capabilities for this class.

Regarding the mAP50 and mAP50-95 metrics, the Yolov5n and Yolov5s models achieved the best performance, respectively. The highest mAP50 value recorded was 66.9%, which is relatively low. Factors such as the quantity and quality of training images, the complexity of the detection task, and the models' capabilities likely contributed to this result. For additional insights, Figure 6 illustrates the average precision values of the different models for detecting saffron plants and weeds. As shown, all models exhibited higher accuracy in detecting saffron plants compared to weeds. Specifically, saffron plants were identified with an average precision ranging from 82.7% to 84.9% across the models, whereas weeds were detected with average precision values between 43.7% and 50.1%.

To further assess the proposed model's performance, the confusion matrix for its detection accuracy across the saffron plant, weed, and background classes is presented in Figure 7. The matrix reveals that the algorithm identified saffron plants in the test images with a high accuracy of 93%. However, its performance in detecting weeds was less effective, as it correctly identified only 59% of the weeds and distinguished them from the background. This limitation may be attributed to the small size of many weeds and their wide size variation in the field. Notably, the algorithm misclassified weeds as saffron plants in just 1% of cases, and no saffron plants were incorrectly identified as weeds—a significant strength of the model. The main error occurred in misclassifying background areas as either saffron plants or weeds.

**Table 2.** Comparison of the performance of different models on saffron field images

Model	No. of layers	No. of parameters	Precision (P)	Recall (R)	mAP50	mAP50-95
Yolov5n	157	1,761,871	0.678	0.655	0.669	0.283
Yolov5s	157	7,015,519	0.689	0.655	0.667	0.284
Yolov5m	291	20,875,359	0.787	0.667	0.655	0.282
Yolov5l	368	46,143,679	0.775	0.654	0.651	0.271
Yolov5x	322	86,180,143	0.679	0.619	0.649	0.276
Proposed	479	3,694,967	0.818	0.674	0.651	0.269

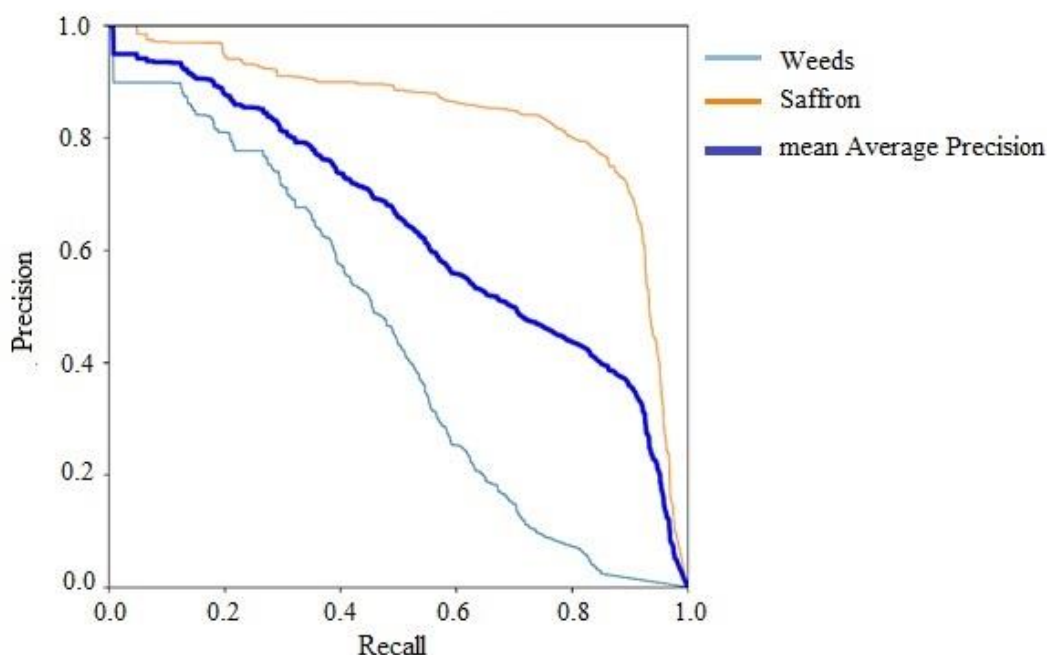


**Figure 5.** Precision-Recall curve of the improved YOLOv5s model

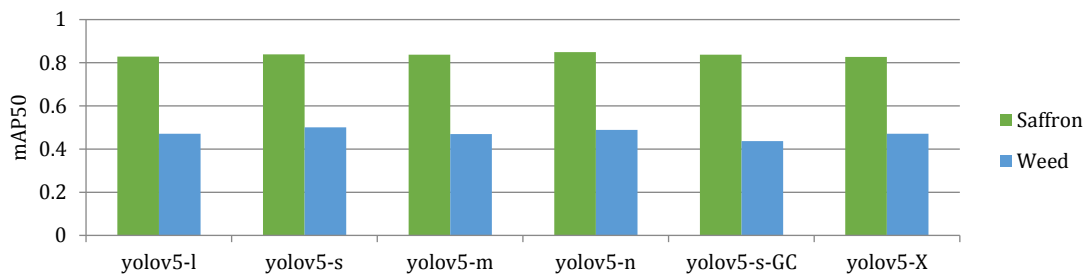


**Figure 6.** Comparison of mAP50 metric values for different models in detecting weeds and saffron plants

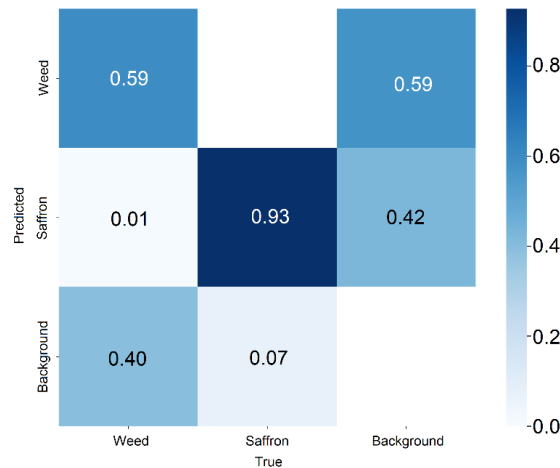


**Figure 7.** Confusion matrix of the improved YOLOv5s model

The superior performance of the proposed YOLO model compared to the baseline YOLOv5 model can be attributed to two key architectural enhancements. The integration of Ghost Bottleneck and C3Ghost modules significantly reduces the number of model parameters, leading to a more computationally efficient network. This translates to faster training and inference times, crucial for real-time weed detection in dynamic agricultural environments. Sonawane and Patil (2024) discuss modifications to the YOLOv5 model, focusing on performance metrics such as precision and recall in weed detection. They highlight the advantages of using advanced architectures for improving detection accuracy and efficiency, which aligns with the architectural enhancements mentioned in this research, such as reducing parameters and enhancing computational efficiency. Narayana and Ramana (2023) show that enhancements in the YOLO v7 architecture can contribute to improved performance metrics (Narayana and Ramana, 2023).

The incorporation of the CoordAtt layer enhances the model's ability to capture spatial information within the feature maps. By considering both channel relationships and positional information, the CoordAtt layer guides the model to focus on relevant regions within the image, resulting in improved detection accuracy and reduced false positives. These combined architectural modifications contribute to the enhanced performance of the proposed model, making it a more suitable and efficient solution for real-time weed detection in saffron fields. Peng et al. (2023) introduced an improved version of the YOLO v7 model that incorporates attention mechanisms to enhance feature extraction for weed detection. Their findings demonstrate significant improvements in mAP metric yield via utilizing the CoordAtt layer in the YOLO architecture (Peng et al., 2023). In another research, modifications in YOLO v8 architecture resulted in improved performance compared to the baseline model, enabling its application for real-time weed detection (Kumar and Misra, 2024).

Besides the strengths of the YOLO models and mainly the modified model proposed in this research, these models suffer from several limitations. Firstly, their performance is heavily

reliant on the quality and quantity of the training data. Limited or biased datasets can hinder generalization and lead to inaccurate detections in real-world scenarios. Secondly, environmental variations, such as changing weather conditions, lighting, and crop growth stages, can significantly impact the model's accuracy and robustness. Furthermore, the model might struggle to accurately detect small weeds or those obscured by crops, potentially leading to missed detections or false positives. Finally, the model's robustness to occlusion, where weeds are partially hidden by other plants or debris, remains a significant challenge. In this regard, developing methods for the model to continuously learn and adapt to changing environmental conditions and different weed species (Adhinata and Sumiharto, 2024; Alif and Hussain, 2024).

#### 4. Conclusions

Advancements in image processing through deep neural networks and the development of object detection algorithms have recently introduced new tools to the agricultural industry. At the heart of these tools are artificial intelligence algorithms that should balance high accuracy with fast detection and decision-making capabilities. The effectiveness and reliability of such algorithms are assessed based on these two parameters. In this study, a weed detection model for saffron fields was developed using the YOLOv5 object detection algorithm. Modifications to the original algorithm focused on reducing the number of parameters and enhancing processing speed compared to its counterpart with the same network width and depth multipliers. Simultaneously, the model's accuracy was improved over existing models. Based on the evaluation results, the proposed model outperformed others in terms of both parameter efficiency and detection accuracy, making it a candidate for integration into robotic systems for selective weed control.

#### Funding declaration

The authors declare that they did not receive funds, grants, or other support for the preparation of this paper.

## Competing interests

No competing financial interests or personal relationships are known to the authors that could have influenced this study.

## References

- Abdullaev, F. I. & Frenkel, G. D. (1999). Saffron in biological and medical research. *Saffron: Crocus Sativus L.*, 103–113.
- Adhinata, F. D. & Sumiharto, R. (2024). A comprehensive survey on weed and crop classification using machine learning and deep learning. *Artificial Intelligence in Agriculture*, 13, 45-63. <https://doi.org/10.1016/j.aia.2024.06.005>
- Admasu, G., Haji, J., Siyum, C., & Ndemo, E. (2024). Impact of Climate Change Adaptation Strategies on Food Security of Farm Households in Rural Dire Dawa Administration, Ethiopia. *Sustainable Agriculture Research*, 13(2), 1-15. <https://doi.org/10.5539/sar.v13n2p1>
- Alif, M. A. R. & Hussain, M. (2024). YOLOv1 to YOLOv10: A comprehensive review of YOLO variants and their application in the agricultural domain. *ArXiv Preprint*. <https://doi.org/10.48550/arXiv.2406.10139>
- Cheng, B., & Matson, E. T. (2015). A feature-based machine learning agent for automatic rice and weed discrimination. *International Conference on Artificial Intelligence and Soft Computing*, 517–527.
- Fernández, J.-A. (2004). *Biology, biotechnology and biomedicine of saffron*.
- Guerrero, J. M., Ruz, J. J. & Pajares, G. (2017). Crop rows and weeds detection in maize fields applying a computer vision system based on geometry. *Computers and Electronics in Agriculture*, 142, 461–472. <https://doi.org/10.1016/j.compag.2017.09.028>
- Hamuda, E., Glavin, M., & Jones, E. (2016). A survey of image processing techniques for plant extraction and segmentation in the field. *Computers and Electronics in Agriculture*, 125, 184–199. <https://doi.org/10.1016/j.compag.2016.04.024>
- Han, K., Wang, Y., Tian, Q., Guo, J., Xu, C., & Xu, C. (2020). Ghostnet: More features from cheap operations. *Proceedings of the IEEE/CVF Conference on Computer Vision and Pattern Recognition*, 1580–1589. <https://doi.org/10.1109/CVPR42600.2020.00165>
- Hou, Q., Zhou, D., & Feng, J. (2021). Coordinate attention for efficient mobile network design. *Proceedings of the IEEE/CVF Conference on Computer Vision and Pattern Recognition*, 13713–13722. <https://doi.org/10.1109/CVPR46437.2021.01350>
- Jeanmart, S., Edmunds, A. J. F., Lamberth, C., & Pouliot, M. (2016). Synthetic approaches to the 2010–2014 new agrochemicals. *Bioorganic & Medicinal Chemistry*, 24(3), 317–341. <https://doi.org/10.1016/j.bmc.2015.12.014>
- José Bagur, M., Alonso Salinas, G. L., Jiménez-Monreal, A. M., Chaouqi, S., Llorens, S., Martínez-Tomé, M., & Alonso, G. L. (2017). Saffron: An old medicinal plant and a potential novel functional food. *Molecules*, 23(1), 30. <https://doi.org/10.3390/molecules23010030>
- Kumar, P., & Misra, U. (2024). Deep Learning for Weed Detection: Exploring YOLO V8 Algorithm's Performance in Agricultural Environments. *2024 2nd International Conference on Disruptive Technologies (ICDT)*, 255–258. <https://doi.org/10.1109/ICDT61202.2024.10489628>
- Kumar, R., Singh, V., Devi, K., Sharma, M., Singh, M. K., & Ahuja, P. S. (2008). State of art of saffron (*Crocus sativus L.*) agronomy: A comprehensive review. *Food Reviews International*, 25(1), 44–85. <https://doi.org/10.1080/87559120802458503>
- Ministry of Agriculture-Jihad. (2020). *Agricultural Statistics, (Vol. II). The Islamic Republic of Iran, Ministry of Agriculture-Jihad, Press. (In Persian)*.
- Narayana, C. L., & Ramana, K. V. (2023). An efficient real-time weed detection technique using YOLOv7. *International Journal of Advanced Computer Science and Applications*, 14(2). <https://doi.org/10.14569/ijacsa.2023.0140265>
- Peng, M., Zhang, W., Li, F., Xue, Q., Yuan, J., & An, P. (2023). Weed detection with improved YOLO v7. *EAI Endorsed Transactions on Internet of Things*, 9(3), e1. <https://doi.org/10.4108/eetiot.v9i3.3468>
- Redmon, J., Divvala, S., Girshick, R., & Farhadi, A. (2016). You only look once: Unified, real-time object detection. In *Proceedings of the IEEE Conference on Computer Vision and Pattern Recognition*, 779-788. <https://doi.org/10.1109/CVPR.2016.91>
- Rodrigo, M. A., Oturan, N., & Oturan, M. A. (2014). Electrochemically assisted remediation of pesticides in soils and water: a review. *Chemical Reviews*, 114(17), 8720–8745. <https://doi.org/10.1021/cr500077e>
- Shahnoushi, N., Abolhassani, L., Kavakebi, V., Reed, M., & Saghaian, S. (2020). Economic analysis of saffron production. In *Saffron* (pp. 337–356). Elsevier. <https://doi.org/10.1016/B978-0-12-818638-1.00021-6>
- Singh, A., Ganapathysubramanian, B., Singh, A. K., & Sarkar, S. (2016). Machine learning for high-throughput stress phenotyping in plants. *Trends in Plant Science*, 21(2), 110–124. <https://doi.org/10.1016/j.tplants.2015.10.015>
- Sonawane, S., & Patil, N. N. (2024). Deep learning-based weed detection in sesame crops using modified YOLOv5 model. *Indian Journal of Weed Science*, 56, 194-199. <http://doi.org/10.5958/0974-8164.2024.00031.X>
- Woyessa, D. (2022). Weed control methods used in agriculture. *American Journal of Life Science and Innovation*, 1(1), 19–26. <https://doi.org/10.54536/ajlsi.v1i1.413>
- Zhou, X., Chen, T., & Zhang, B. (2023). Research on the impact of digital agriculture development on agricultural green total factor productivity. *Land*, 12(1), 195. <https://doi.org/10.3390/land12010195>

## Data availability statement

The data supporting the results of this study are available from the corresponding author upon reasonable request.